APPLICATION OF LES TURBULENCE MODEL TO MOTORED 4-STROKE INTERNAL COMBUSTION ENGINE

Oldřich Vítek*, Bohumil Mareš† Jan Macek‡

Czech Technical University in Prague, Josef Božek Research Center, Prague

Abstract

The presented paper is purely a theoretical study – commercial CFD code FIRE is used as a main simulation tool. The paper deals with application of simple LES model (Smagorinsky) to a case of motored (no combustion) small SI engine. In total, 45 consecutive engine cycles ware calculated using moderately coarse mesh (typical cell size is 1.0mm). These data ware statistically evaluated including the time evolution of statistical properties. Statistically averaged cycle is directly compared with RANS calculation using the same mesh. Examples of flow-fields are presented at different piston positions to compare LES with RANS.

1 Introduction

Turbulence modelling is still important issue when detailed CFD calculations of internal combustion engine (ICE) are performed. The LES approach (e.g. [3, 7, 10–12, 14, 16]) seems to be a promising way to improve the accuracy of the results. However, the application to ICE causes a lot of difficulties and problems.

This is a purely theoretical study to test basic performance of simple LES model (Smagorinsky algebraic model [13]) under conditions of motored (no combustion) 4-stroke engine. The first target is to evaluate statistical convergence – in other words, how many cycles need to be calculated to obtain proper averaged values. The second target is to compare these averaged results with pure RANS calculations (two different RANS turbulence models are considered).

2 Theoretical Background

The mathematical model is based on standard CFD approach applied in commercial codes – in this case, the FIRE code [1] is selected as main simulation tool. The model itself is based on non-stationary 3-D compressible equation set (integral formulation) which is

*Ing., Ph.D., e-mail: Oldrich.Vitek@fs.cvut.cz
†Ing., Ph.D., e-mail: Bohumil.Mares@fs.cvut.cz
‡Prof. Ing., DrSc., e-mail: Jan.Macek@fs.cvut.cz

filtered either in space domain (and closed by LES turbulence model) or in time domain (and closed by RANS turbulence model). Details can be found in FIRE manuals [1].

The statistical evaluation of LES results is based on ensemble averaging which is generally defined in Equation 1 (more details can be found in [15]), f^n corresponds to the n-th realization of the same experiment (n is index only).

$$F^{avg}(x_i,t) = \lim_{N\to\infty} \frac{1}{N} \sum_{n=1}^{N} f^n(x_i,t) \tag{1}$$

In the case of internal combustion engine, each 'experiment realization' (total number of experiments is given by N) is represented by means of one engine cycle. As the ICE works periodically, it makes sense to define the averaging procedure by Equation set 2 – the time variable t is replaced by angle variable α (due to periodicity it makes sense to define $\alpha \in \langle 0; 4\pi \rangle$ and use the angle definition of $\alpha + (n-1)\,4\pi$ for the n-th engine cycle), the cycle period is represented by the angle of 4π (4-stroke engine – 2 revolutions represent 1 engine cycle). All engine cycles are calculated consecutively – the results of previous cycle directly influence those of the following cycle.

$$F^{avg}(x_i,\alpha) = \frac{1}{N} \sum_{n=1}^{N} f^n\big(x_i, \alpha + (n-1)\,4\pi\big) \tag{2a}$$

$$F^{rms}(x_i,\alpha) = \sqrt{\frac{\sum_{n=1}^{N} \Big(f^n\big(x_i, \alpha + (n-1)\,4\pi\big) - F^{avg}(x_i,\alpha)\Big)^2}{N}} \tag{2b}$$

The above mentioned averaging approach is applied to velocity vectors only (as the data evaluation is quite time consuming process), hence $f^n = u_i$. Ensemble averaged turbulence kinetic energy corresponds to *rms* values of all velocity vector components $k = \frac{1}{2} u_i^{rms} u_i^{rms}$.

However, the ensemble averaging (it is described in [15] as the most general type of Reynolds averaging) may cause a problem when applied to a case of ICE. The main reason is the fact, that in the case of multi-cylinder engine there is a 'low frequency' interaction (the process is slower when compared with engine basic frequency which corresponds to engine speed) among all those cylinders. This causes slow fluctuations of all flow properties. If averaging (Equation set 2) is applied, these slow fluctuations directly influence the *rms* value and hence, it is considered to be a turbulence. However, it should be stressed that it is difficult to filter out these slow fluctuations to get rid of this problem. Moreover, in the presented case only one-cylinder engine is consider (and the initialization procedure of both intake and exhaust ports is always the same) – therefore, the problem is not present in this case.

3 Computed Cases

This paper deals with application of very simple Smagorinsky LES model [13] to a case of 4-stroke small passenger car SI engine in motored regime (no combustion, no fuel injection). As the LES approach leads to a particular realization of flow field during engine cycle

(unlike the case of RANS approach when averaged flow field is supposed to be predicted), many consecutive cycles has to be calculated and statistically evaluated to obtain averaged values. These results are compared with RANS calculation using the same mesh. Two different RANS turbulence models were tested – standard $k-\epsilon$ (e.g. [8,9]) and $k-\zeta-f$ (e.g. [2,6]). Main mesh parameters are summarized in Table 1. The authors are aware of the fact that the applied mesh might be a bit coarse for LES calculations while it is a bit too fine for RANS simulations. On the other hand, PANS simulations (for more details see [4,5]) combine both approaches – it is planned to apply PANS approach to engine simulations to keep LES features in important areas while having coarse mesh (hence RANS approach is applied) in less important domains. This can significantly decrease computation time. Based on that, it makes sense to compare RANS applied on relatively fine mesh (in terms of RANS approach) with LES on the same mesh.

Parameter	Unit	Value	
Typical Cell Size	$[mm]$	1.0	
Minimum Number of Cells	$[1]$	1.08	10^6
Maximum Number of Cells	$[1]$	2.82	10^6
Total Amount of Mesh Sets	$[1]$	77	
Maximum Angle Interval of Single Mesh Set	$[degCA]$	10	

Table 1: Main mesh parameters.

Main engine parameters are presented in Table 2. The engine model (Figure 1) is based on existing 4-stroke port-injection small SI engine – all geometrical data including valve lift profiles are taken from the real engine. As it is purely theoretical work, there is no comparison with experimental data (this is planned for future). To speed up calculation, relatively high engine speed (5500 rpm) was selected.

Parameter	Unit	Value
Bore	$[mm]$	79.0
Stroke	$[mm]$	74.0
Engine Speed	$[min^{-1}]$	5500
Fuel Injection		Indirect (into ports)
Intake Valve Open	$[degCA]$	342
Intake Valve Close	$[degCA]$	610
Exhaust Valve Open	$[degCA]$	842
Exhaust Valve Close	$[degCA]$	390

Table 2: Main engine parameters.

It should be stressed that engine geometry is not symmetrical with respect to plane YZ (Figure 1). This is caused by the design of exhaust port. However, all remaining engine geometry is symmetrical with respect to that plane (YZ). Based on that, when looking at some results (mainly those which use the cutting plane which is perpendicular to Y-axis – e.g. Figure 4 or Figure 11), they may seem to be symmetrical however they are not. On

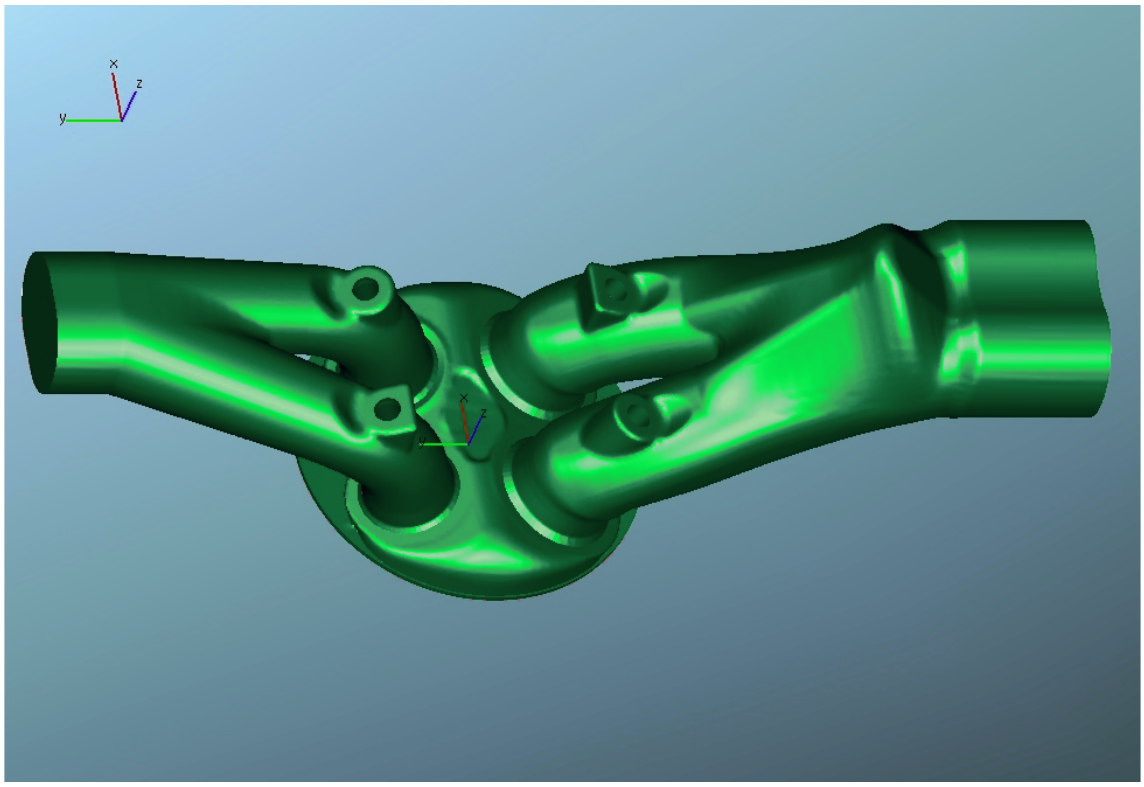

Figure 1: Engine geometry corresponding to top dead center (TDC) during gas exchange phase of 4-stroke engine (all valves are open hence both exhaust port (left) and intake one (right) are included in calculation geometry); due to design of exhaust port, the geometry is not symmetrical (when exhaust port is removed, the geometry is symmetrical with respect to plane YZ).

the other hand, the non-symmetry (due to exhaust port) influences exhaust stroke and early intake stroke (as there is non-zero valve overlap). Once the exhaust port is removed from the calculation (exhaust valves are closed), the solution tends to return to the symmetry quite quickly – this applies to both RANS and averaged LES.

Regarding calculation set-up, no details are presented as the standard setting (based on recommendation from AVL support staff) is applied. The main important information is presented in Table 3. The most important issue is the time step selection. For RANS calculations, maximum time step is 1 degCA while for LES simulations, it is set to value of 0.1 degCA. The authors are aware of the fact that there is empirically based recommendation that for proper LES simulation, the time step should correspond to CFL=1 ($\Delta t = \frac{CFL}{\frac{|w_i|+a}{\Delta x_i}}$). Based on that, the applied time step is a bit longer (especially during compression/expansion phase) – there is some kind of filtering in time domain due to selection of the time step. The main reason for selecting the longer time step is the calculation time as the LES approach is generally very time consuming. Both the intake port and exhaust one are 'added' to computational domain only when corresponding valves are open. It is clear that the information is lost during the phase when port is removed from calculation. The port initial conditions (homogeneous ones) are always the same (regardless of cycle number) and are applied in the first time step when the port is attached to computa-

Parameter	Unit	LES Smagorinsky	RANS $k-\zeta-f$	RANS $k-\epsilon$
Maximum Time Step	$[degCA]$	0.1	1.0	1.0
Calculated Consecutive Cycles	$[-]$	45	5	5
Averaging Procedure Applied		Yes	No	No
Avg. Procedure Cycle Step	$[-]$ (*cycles*)	5	–	–
Avg. Procedure Angle Step	$[degCA]$	45	–	–
Num. Accuracy: Continuity		2nd order	2nd order	2nd order
Num. Accuracy: Momentum		2nd order	2nd order	2nd order
Num. Accuracy: Energy		1st order	1st order	1st order
Num. Accuracy: Turbulence		1st order	1st order	1st order

Table 3: Main calculation set-up parameters.

tional domain (this happens when the corresponding valves are opened for the first time) – this procedure is usually called re-initialization. The authors are aware of the fact that for proper LES calculation (to keep all vortex structures), the ports have to be part of the computational domain even if the corresponding valves are closed – this was skipped due to both computational time (to reduce it as much as possible) and the fact that the influence on the flow field in the cylinder is relatively minor. It should be stressed that 5 consecutive cycles were calculated for RANS cases to get periodic solution (in other words – to avoid the influence of estimated initial conditions). However, no averaging procedure was applied – instead, the results from the last cycle (the 5th one) were considered to be the final one (the AVL's recommendation is to calculate at least 2-3 cycles for RANS to get the periodic solution).

4 Result Discussion

Due to enormous amount of calculated data (over 4.5TB for all 45 cycles of LES data) and due to limited size of this PDF file, only some results are presented. These results were selected to have the most important qualitative properties so that the reader can get all important information.

The first set of results is shown in Figures 2-9. Figures 2-5 correspond to late intake stroke while Figures 6-9 represent early exhaust stroke. The main reason to present these data is to show the statistical convergence of averaged LES solution. As it is well known, at least 10-15 cycles are need to obtain statistical convergence for averaged velocity field (there is little difference among the results in subfigures 2.3-2.9). On the other hand, significantly more cycles are required to statistically converge the 2nd-order statistical moments (in this case, the averaged turbulence kinetic energy represents a sum of 3 statistical moments of the 2nd-order as it is defined in Equation 2b). There are still visible small differences in averaged turbulence kinetic energy between the subfigure 3.8 and 3.9 – in this sense, it may be necessary to calculate even more cycles to obtain fully converged statistical moments of the 2nd-order. From practical point of view, the difference between results averaged after 40 cycles and those averaged after 45 cycles is relatively small. This conclusion is supported by data presented in Figures 4-5 which correspond to different cutting plane when compared with Figures 2-3 (see Figure 1 for coordinate system orientation). From qualitative point of view, the same applies to data presented in Figures 6-9. Another interesting feature is the fact, that both velocity vector magnitude field and turbulence kinetic energy one seem almost the same when averaging is applied after 15 and 20 cycles (subfigure 2.3 and 2.4; subfigure 3.3 and 3.4). However, once the averaging is applied after more cycles, there are visible changes in averaged values (this mainly applies to higher order statistical moments, e.g. turbulence kinetic energy). The results were checked once again to be sure that no procedural error was made. There seems to be a misleading convergence of statistical properties when 15-20 cycles are calculated. Based on that, it is recommended to calculate at least 25 cycles to obtain statistically converged velocity vector field (1st-order statistical moment) or at least 40 cycles to get statistical convergence for 2nd-order statistical moments (e.g. turbulence kinetic energy).

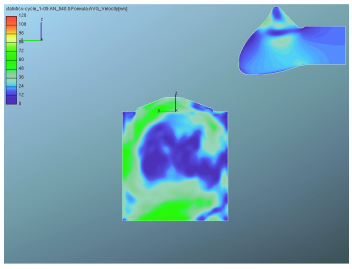

Subfigure 2.1: averaging after 5 engine cycles

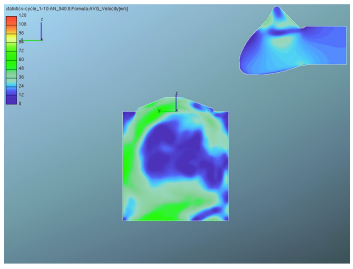

Subfigure 2.2: averaging after 10 engine cycles

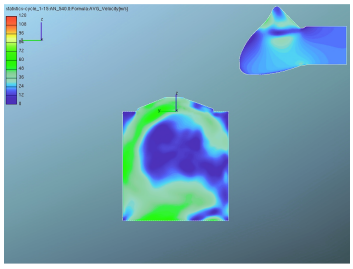

Subfigure 2.3: averaging after 15 engine cycles

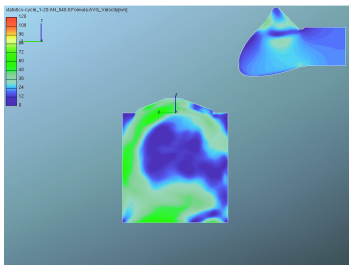

Subfigure 2.4: averaging after 20 engine cycles

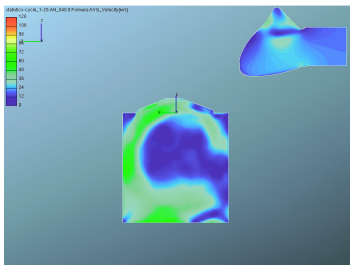

Subfigure 2.5: averaging after 25 engine cycles

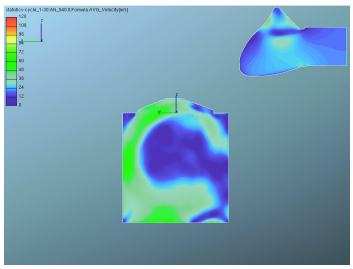

Subfigure 2.6: averaging after 30 engine cycles

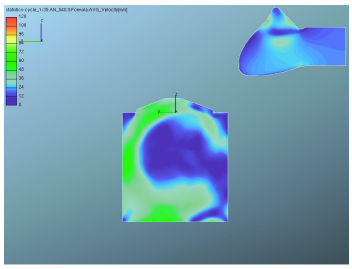

Subfigure 2.7: averaging after 35 engine cycles

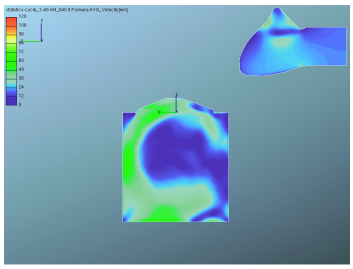

Subfigure 2.8: averaging after 40 engine cycles

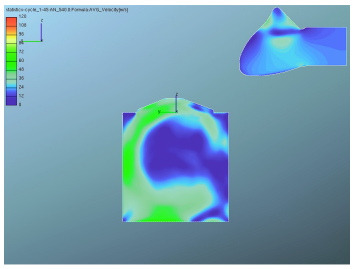

Subfigure 2.9: averaging after 45 engine cycles

Figure 2: Averaged velocity vector magnitude for LES case at crank angle 540 degCA (late intake stroke) – dependence on the amount of engine cycles used for averaging procedure (cutting plane perpendicular to X-axis – see Figure 1 for coordination system orientation).

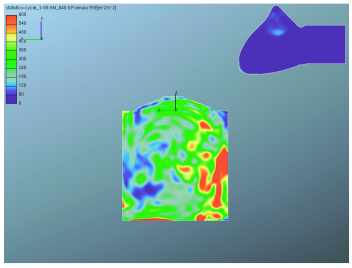

Subfigure 3.1: averaging after 5 engine cycles

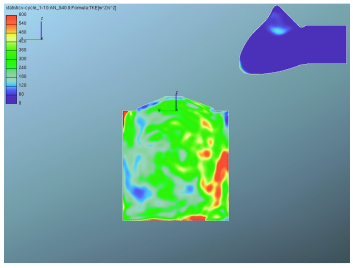

Subfigure 3.2: averaging after 10 engine cycles

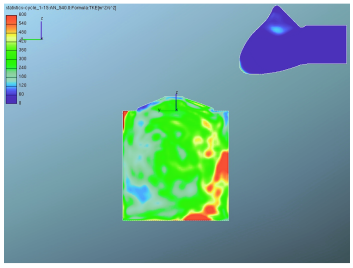

Subfigure 3.3: averaging after 15 engine cycles

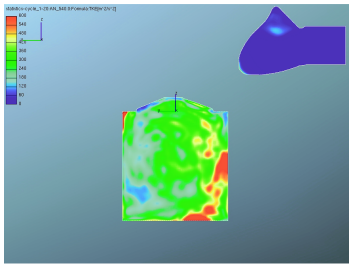

Subfigure 3.4: averaging after 20 engine cycles

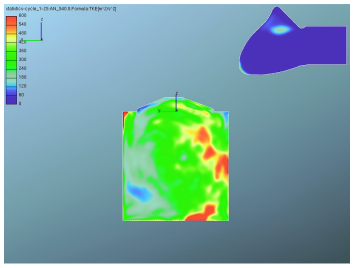

Subfigure 3.5: averaging after 25 engine cycles

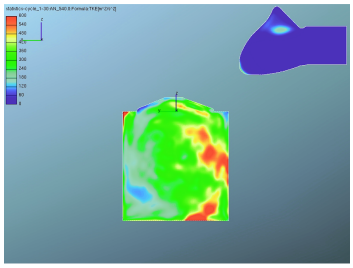

Subfigure 3.6: averaging after 30 engine cycles

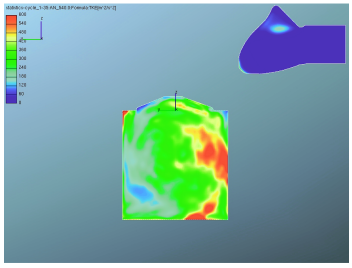

Subfigure 3.7: averaging after 35 engine cycles

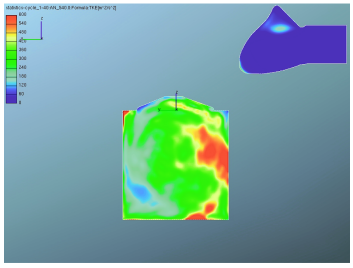

Subfigure 3.8: averaging after 40 engine cycles

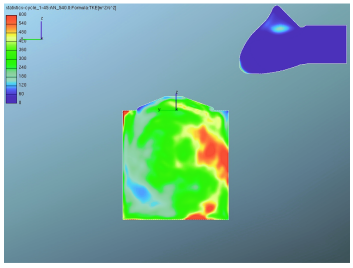

Subfigure 3.9: averaging after 45 engine cycles

Figure 3: Averaged turbulence kinetic energy time evolution for LES case at crank angle 540 degCA (late intake stroke) – dependence on the amount of engine cycles used for averaging procedure (cutting plane perpendicular to X-axis – see Figure 1 for coordination system orientation).

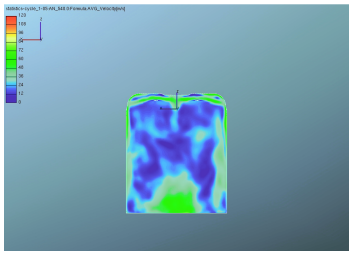

Subfigure 4.1: averaging after 5 engine cycles

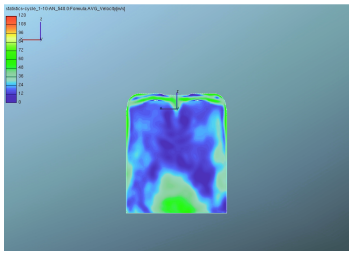

Subfigure 4.2: averaging after 10 engine cycles

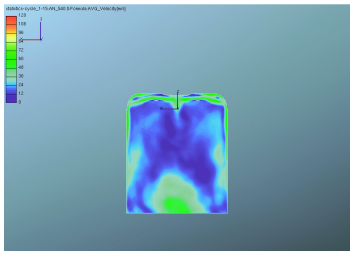

Subfigure 4.3: averaging after 15 engine cycles

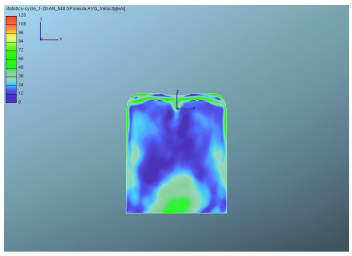

Subfigure 4.4: averaging after 20 engine cycles

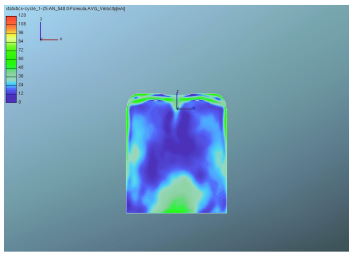

Subfigure 4.5: averaging after 25 engine cycles

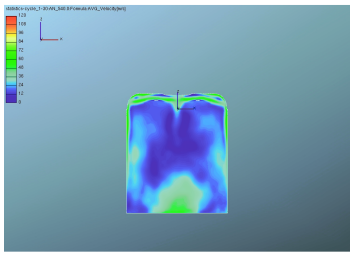

Subfigure 4.6: averaging after 30 engine cycles

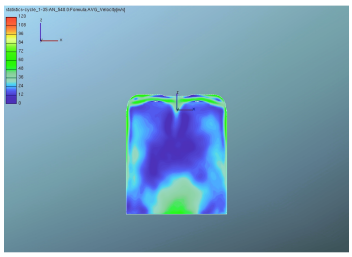

Subfigure 4.7: averaging after 35 engine cycles

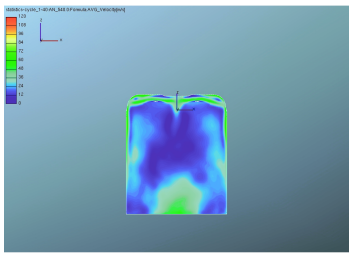

Subfigure 4.8: averaging after 40 engine cycles

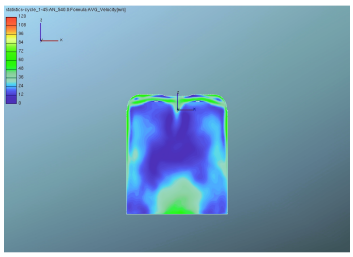

Subfigure 4.9: averaging after 45 engine cycles

Figure 4: Averaged velocity vector magnitude for LES case at crank angle 540 degCA (late intake stroke) – dependence on the amount of engine cycles used for averaging procedure (cutting plane perpendicular to Y-axis – see Figure 1 for coordination system orientation).

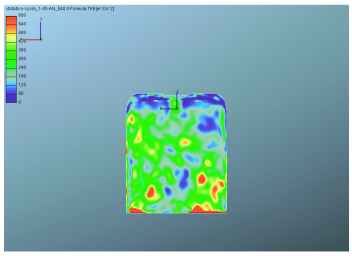

Subfigure 5.1: averaging after 5 engine cycles

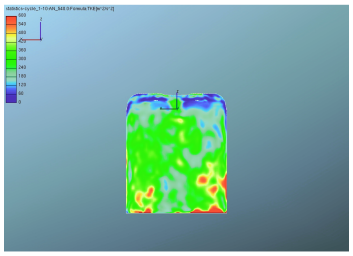

Subfigure 5.2: averaging after 10 engine cycles

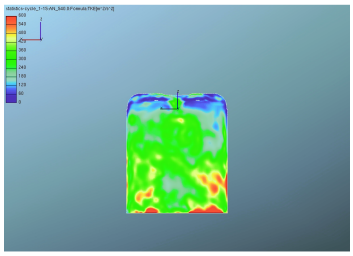

Subfigure 5.3: averaging after 15 engine cycles

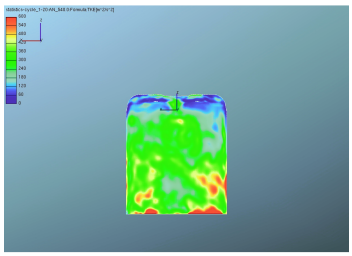

Subfigure 5.4: averaging after 20 engine cycles

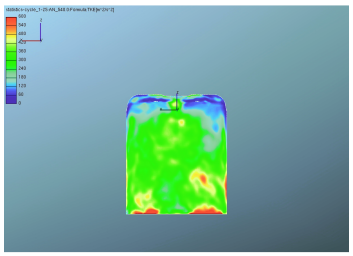

Subfigure 5.5: averaging after 25 engine cycles

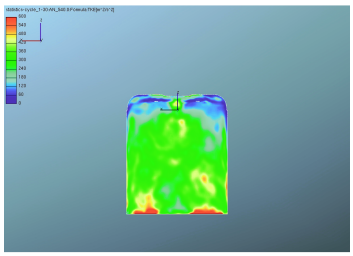

Subfigure 5.6: averaging after 30 engine cycles

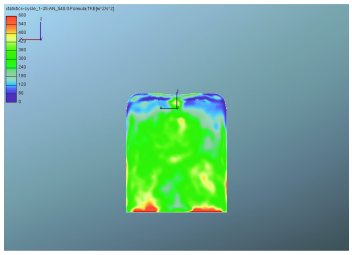

Subfigure 5.7: averaging after 35 engine cycles

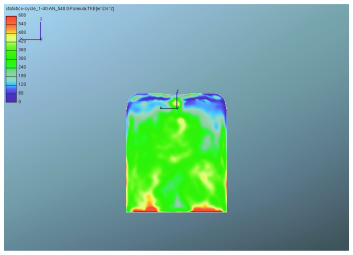

Subfigure 5.8: averaging after 40 engine cycles

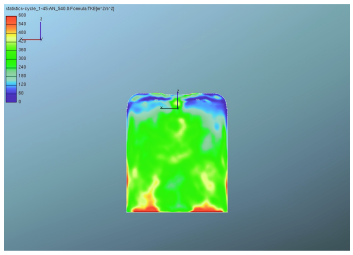

Subfigure 5.9: averaging after 45 engine cycles

Figure 5: Averaged turbulence kinetic energy time evolution for LES case at crank angle 540 degCA (late intake stroke) – dependence on the amount of engine cycles used for averaging procedure (cutting plane perpendicular to Y-axis – see Figure 1 for coordination system orientation).

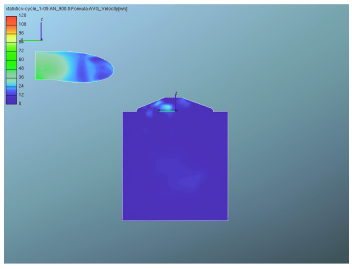

Subfigure 6.1: averaging after 5 engine cycles

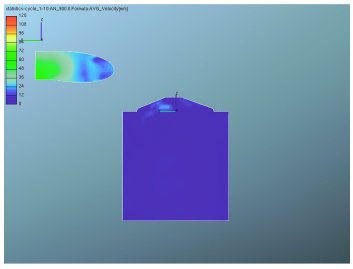

Subfigure 6.2: averaging after 10 engine cycles

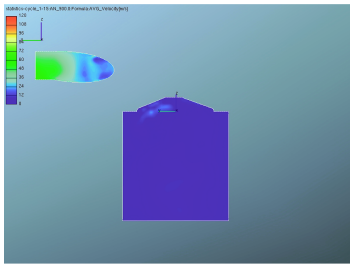

Subfigure 6.3: averaging after 15 engine cycles

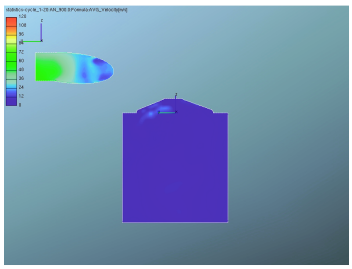

Subfigure 6.4: averaging after 20 engine cycles

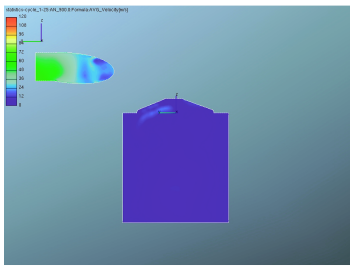

Subfigure 6.5: averaging after 25 engine cycles

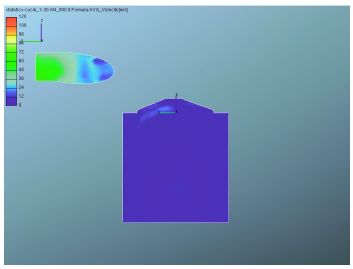

Subfigure 6.6: averaging after 30 engine cycles

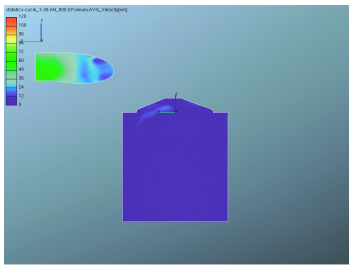

Subfigure 6.7: averaging after 35 engine cycles

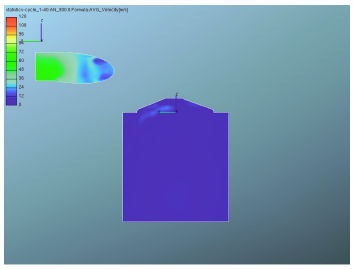

Subfigure 6.8: averaging after 40 engine cycles

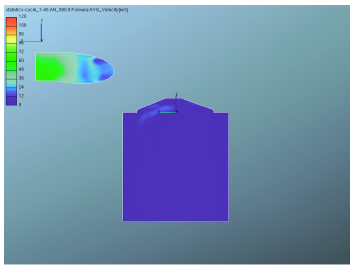

Subfigure 6.9: averaging after 45 engine cycles

Figure 6: Averaged velocity vector magnitude for LES case at crank angle 900 degCA (early exhaust stroke)– dependence on the amount of engine cycles used for averaging procedure (cutting plane perpendicular to X-axis – see Figure 1 for coordination system orientation).

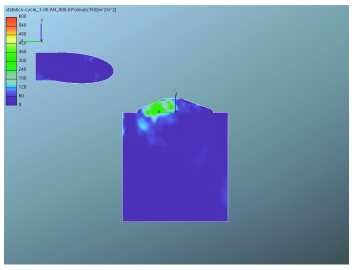

Subfigure 7.1: averaging after 5 engine cycles

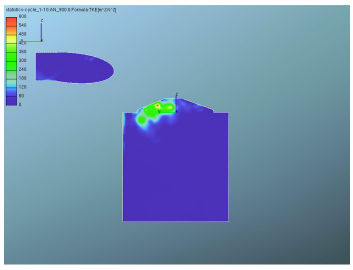

Subfigure 7.2: averaging after 10 engine cycles

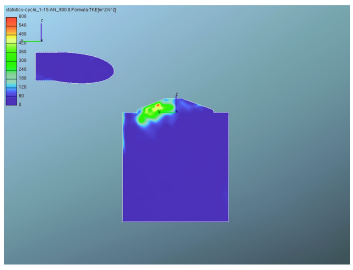

Subfigure 7.3: averaging after 15 engine cycles

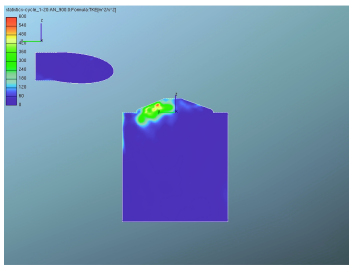

Subfigure 7.4: averaging after 20 engine cycles

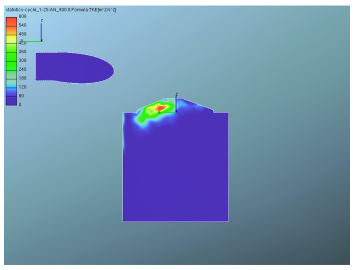

Subfigure 7.5: averaging after 25 engine cycles

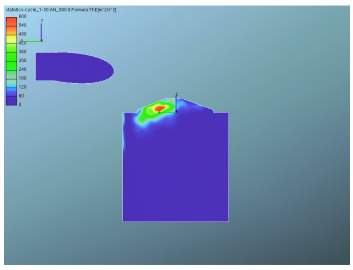

Subfigure 7.6: averaging after 30 engine cycles

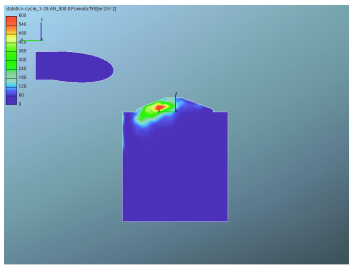

Subfigure 7.7: averaging after 35 engine cycles

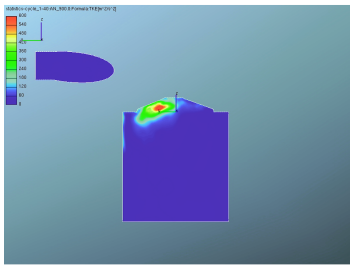

Subfigure 7.8: averaging after 40 engine cycles

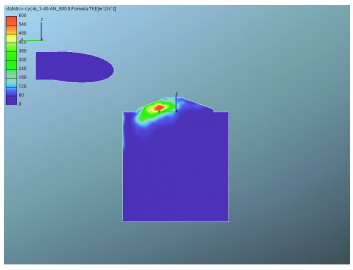

Subfigure 7.9: averaging after 45 engine cycles

Figure 7: Averaged turbulence kinetic energy time evolution for LES case at crank angle 900 degCA (early exhaust stroke) – dependence on the amount of engine cycles used for averaging procedure (cutting plane perpendicular to X-axis – see Figure 1 for coordination system orientation).

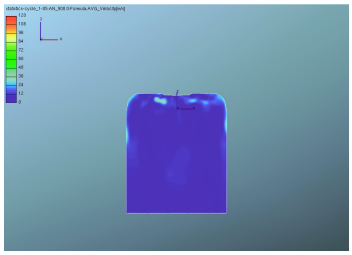

Subfigure 8.1: averaging after 5 engine cycles

Subfigure 8.2: averaging after 10 engine cycles

Subfigure 8.3: averaging after 15 engine cycles

Subfigure 8.4: averaging after 20 engine cycles

Subfigure 8.5: averaging after 25 engine cycles

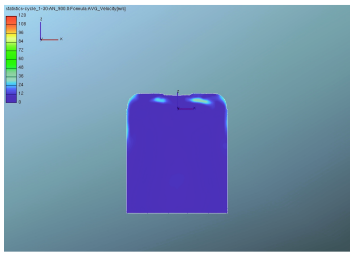

Subfigure 8.6: averaging after 30 engine cycles

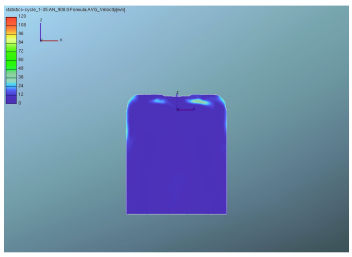

Subfigure 8.7: averaging after 35 engine cycles

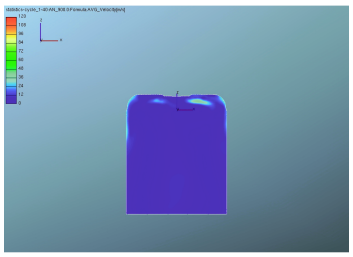

Subfigure 8.8: averaging after 40 engine cycles

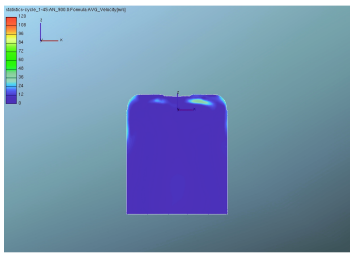

Subfigure 8.9: averaging after 45 engine cycles

Figure 8: Averaged velocity vector magnitude for LES case at crank angle 540 degCA (early exhaust stroke) – dependence on the amount of engine cycles used for averaging procedure (cutting plane perpendicular to Y-axis – see Figure 1 for coordination system orientation).

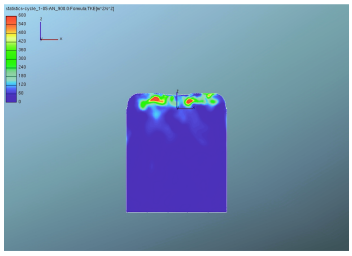

Subfigure 9.1: averaging after 5 engine cycles

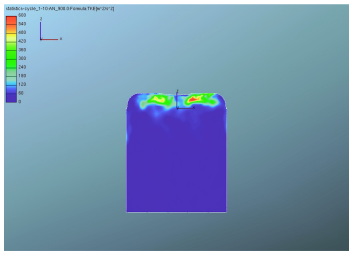

Subfigure 9.2: averaging after 10 engine cycles

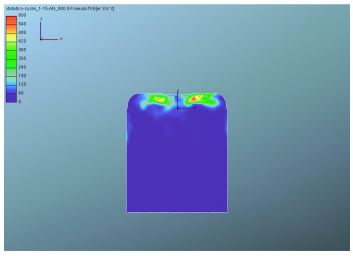

Subfigure 9.3: averaging after 15 engine cycles

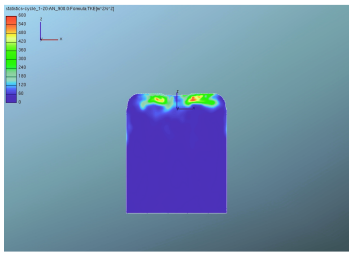

Subfigure 9.4: averaging after 20 engine cycles

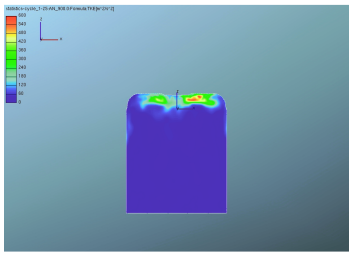

Subfigure 9.5: averaging after 25 engine cycles

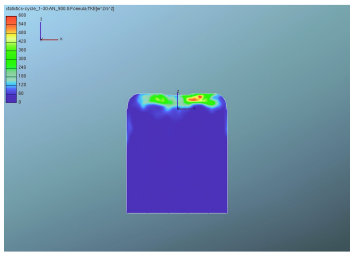

Subfigure 9.6: averaging after 30 engine cycles

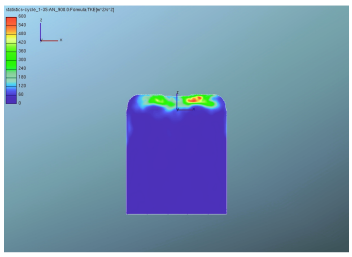

Subfigure 9.7: averaging after 35 engine cycles

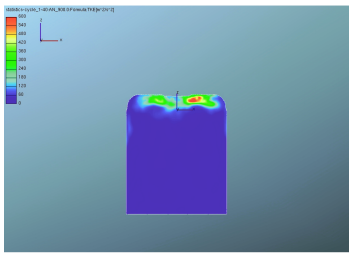

Subfigure 9.8: averaging after 40 engine cycles

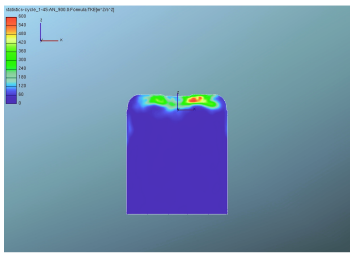

Subfigure 9.9: averaging after 45 engine cycles

Figure 9: Averaged turbulence kinetic energy time evolution for LES case at crank angle 540 degCA (early exhaust stroke) – dependence on the amount of engine cycles used for averaging procedure (cutting plane perpendicular to Y-axis – see Figure 1 for coordination system orientation).

The second set of results is shown in Figures 10-15. These results compare different turbulence models at the same crank position. As it was mentioned above, it is purely theoretical study. No measurements are available that is why it is not possible to decide which model is the superior one. Based on that, only qualitative comparison of applied turbulence models is possible. On the other hand, the LES simulation set-up respects recommended values (concerning mainly the mesh size, the time step and sufficient number of consecutive cycles) so that it is reasonable to believe that LES should have the best ability to predict. This statement is supported by the well know fact that RANS 2-equation turbulence models are not accurate when applied in internal combustion engines (ICE). The applied RANS models differ significantly, the AVL (the developer of FIRE code) recommends the $k - \zeta - f$ model for engine application. The standard $k - \epsilon$ was selected to test the performance of the old well-known RANS model. As it is clear from the figures, the averaged velocity vector magnitude field is relatively similar for all applied turbulence models. On the other hand, there are significant differences in predicted turbulence kinetic energy. The authors are aware of the fact that the RANS approach is based on time averaging while the averaged LES is based on ensemble averaging (Equation 2). These two approaches are not the same, especially for the case of ICE (periodic solution). On the other hand, it is usually expected that the difference between those is relatively small. This statement is supported by the results of averaged velocity vector magnitude (left column in the Figures 10-15). Based on that, the difference in predicted turbulence kinetic energy seem to be too large. Even from qualitative point of view, the results are quite different. Generally speaking, the averaged LES approach predicts significantly higher levels of turbulence kinetic energy – this statement holds especially for the regions with expected high levels of turbulence. When comparing both RANS models, they seem to be reasonably similar. The standard $k - \epsilon$ has a bit higher peaks of turbulence kinetic energy. Another feature of the standard $k - \epsilon$ model is that its solution tends to return to symmetry faster (once the geometry is symmetrical) when compared with the $k - \zeta - f$ – Figures 11 and 13. In this sense, it is similar to the averaged LES approach.

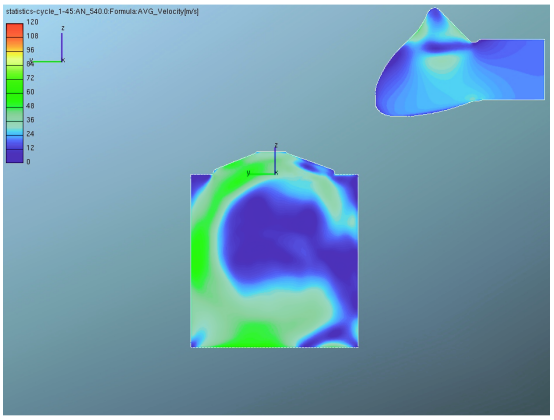

Subfigure 10.1: LES (Smagorinsky) – averaged velocity magnitude

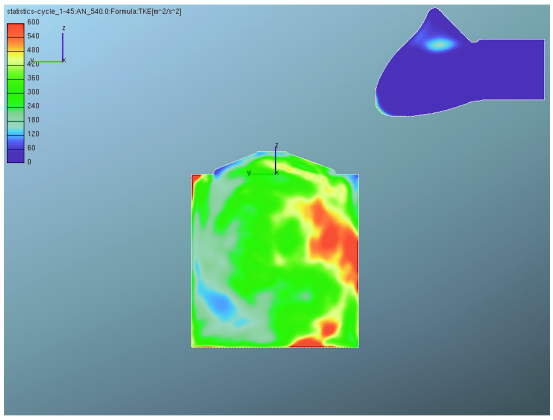

Subfigure 10.2: LES (Smagorinsky) – averaged turbulence kinetic energy

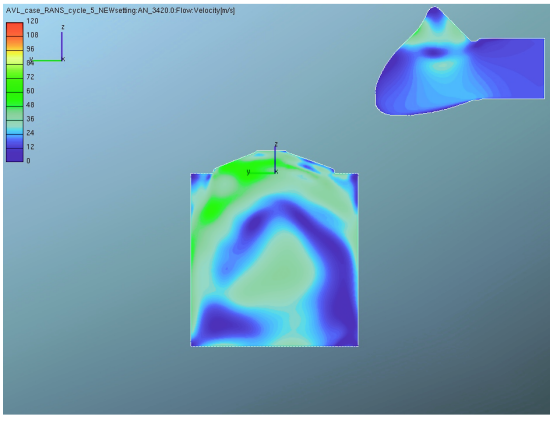

Subfigure 10.3: RANS ($k-\zeta-f$) – velocity magnitude

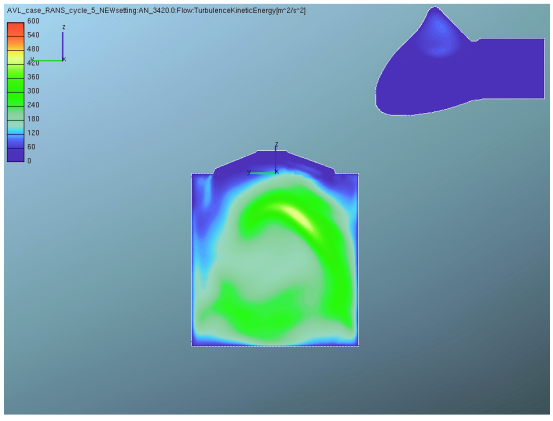

Subfigure 10.4: RANS ($k-\zeta-f$) – turbulence kinetic energy

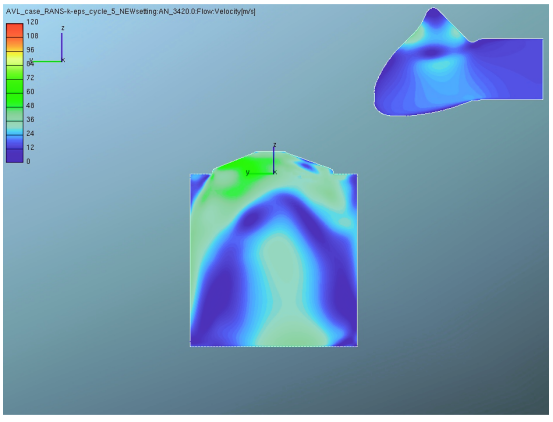

Subfigure 10.5: RANS ($k-\epsilon$) – velocity magnitude

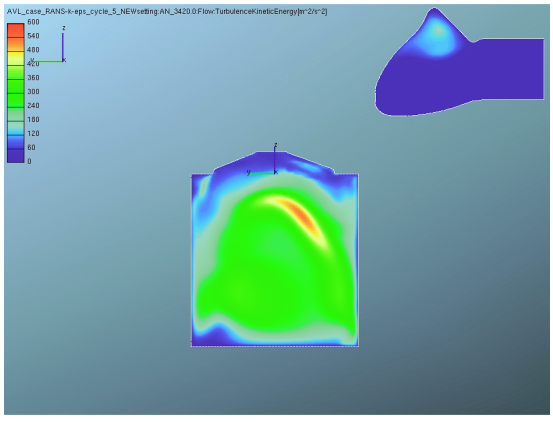

Subfigure 10.6: RANS ($k-\epsilon$) – turbulence kinetic energy

Figure 10: Comparison of different turbulence models at crank angle of 540 degCA (late intake stroke) – averaged velocity magnitude is plotted in left column while turbulence kinetic energy is placed in right column (cutting plane perpendicular to X-axis – see Figure 1 for coordination system orientation).

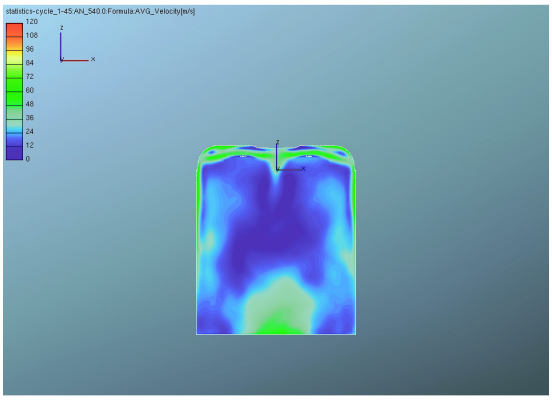

Subfigure 11.1: LES (Smagorinsky) – averaged velocity magnitude

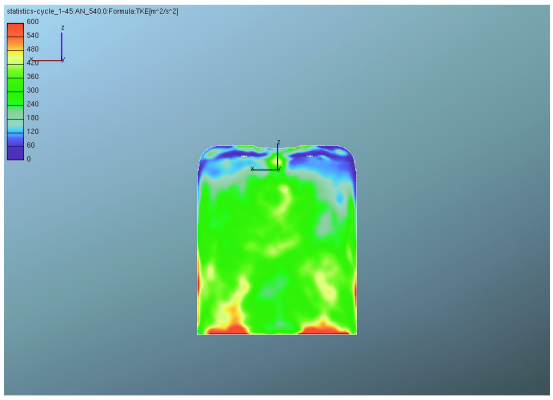

Subfigure 11.2: LES (Smagorinsky) – averaged turbulence kinetic energy

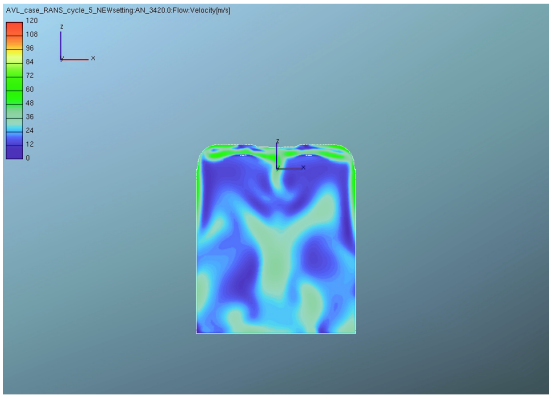

Subfigure 11.3: RANS ($k-\zeta-f$) – velocity magnitude

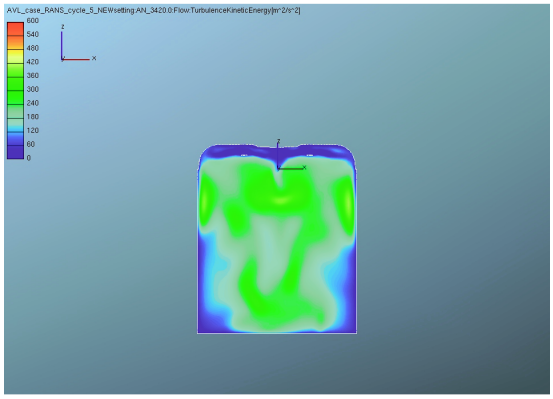

Subfigure 11.4: RANS ($k-\zeta-f$) – turbulence kinetic energy

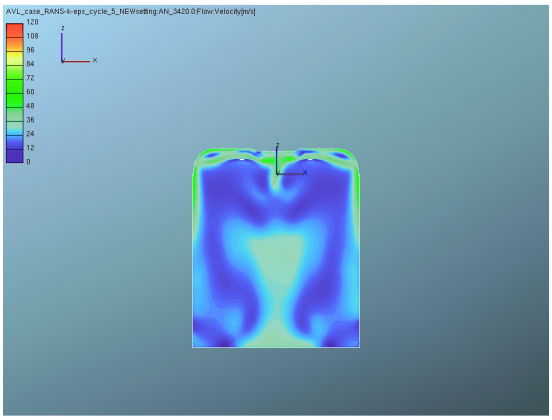

Subfigure 11.5: RANS ($k-\epsilon$) – velocity magnitude

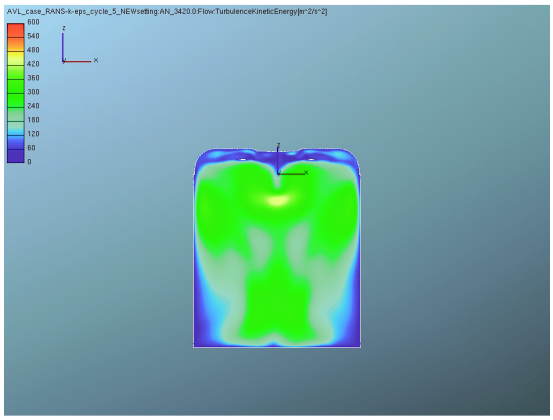

Subfigure 11.6: RANS ($k-\epsilon$) – turbulence kinetic energy

Figure 11: Comparison of different turbulence models at crank angle of 540 degCA (late intake stroke) – averaged velocity magnitude is plotted in left column while turbulence kinetic energy is placed in right column (cutting plane perpendicular to Y-axis – see Figure 1 for coordination system orientation).

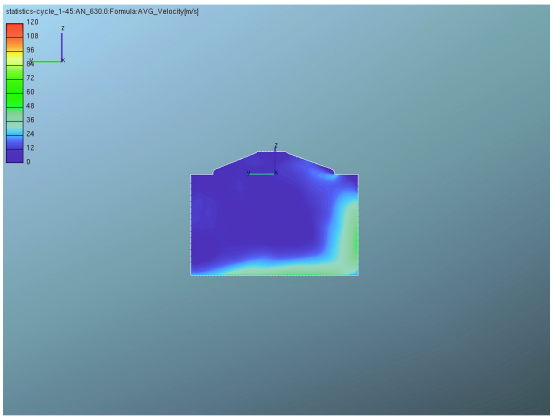

Subfigure 12.1: LES (Smagorinsky) – averaged velocity magnitude

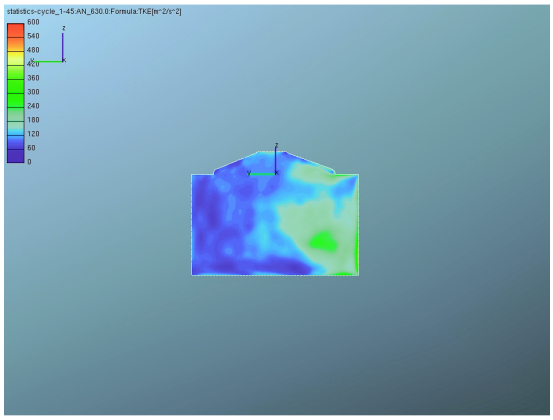

Subfigure 12.2: LES (Smagorinsky) – averaged turbulence kinetic energy

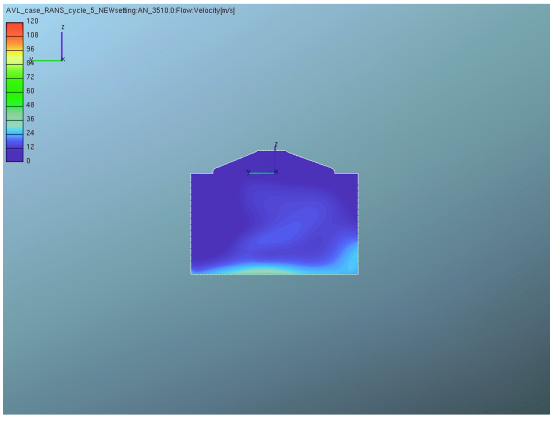

Subfigure 12.3: RANS ($k-\zeta-f$) – velocity magnitude

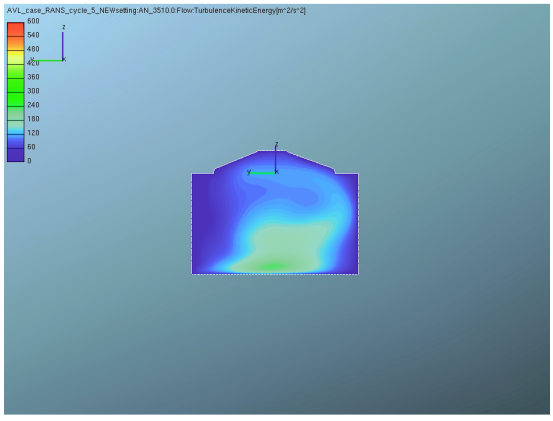

Subfigure 12.4: RANS ($k-\zeta-f$) – turbulence kinetic energy

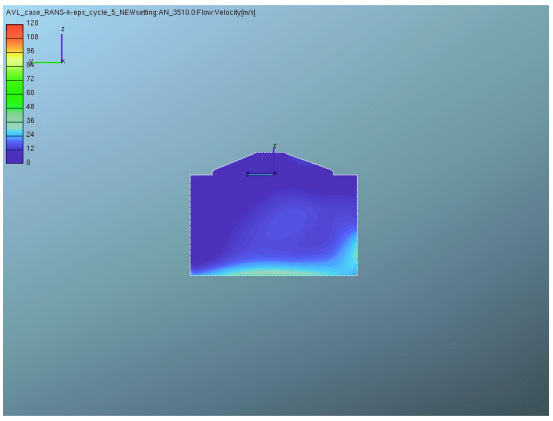

Subfigure 12.5: RANS ($k-\epsilon$) – velocity magnitude

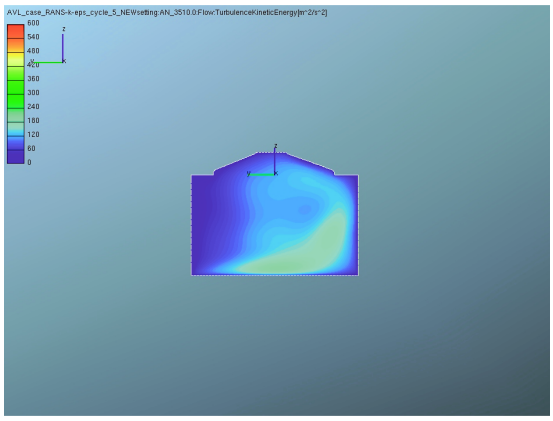

Subfigure 12.6: RANS ($k-\epsilon$) – turbulence kinetic energy

Figure 12: Comparison of different turbulence models at crank angle of 630 degCA (early compression stroke) – averaged velocity magnitude is plotted in left column while turbulence kinetic energy is placed in right column (cutting plane perpendicular to X-axis – see Figure 1 for coordination system orientation).

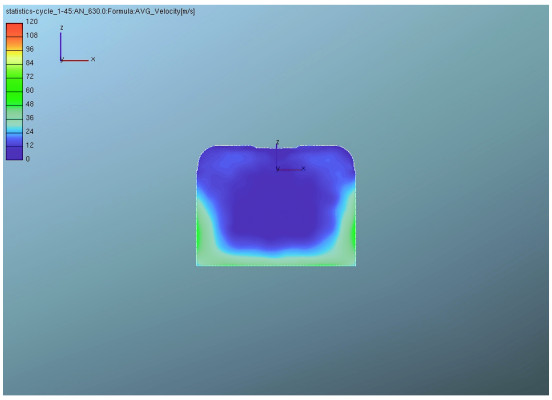

Subfigure 13.1: LES (Smagorinsky) – averaged velocity magnitude

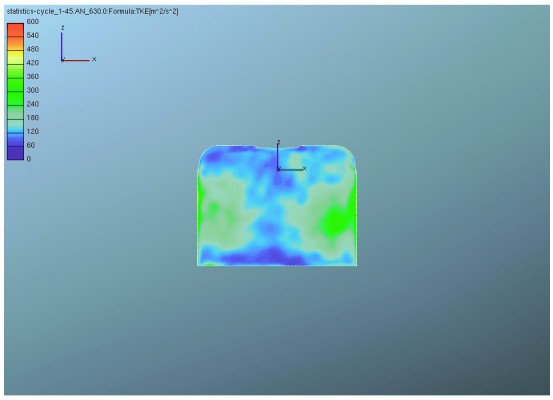

Subfigure 13.2: LES (Smagorinsky) – averaged turbulence kinetic energy

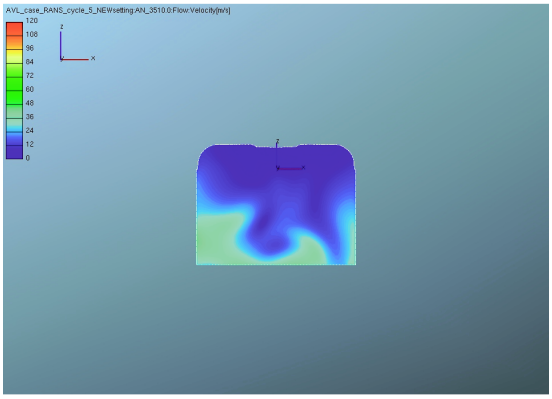

Subfigure 13.3: RANS ($k-\zeta-f$) – velocity magnitude

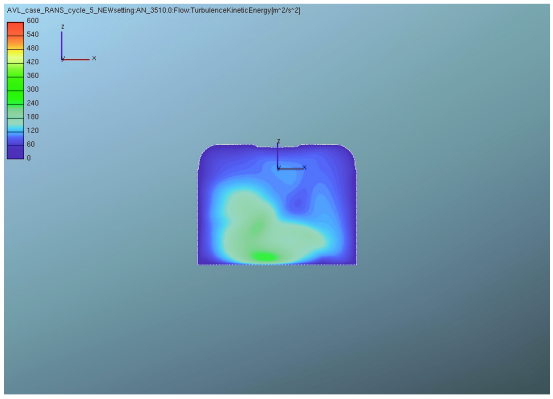

Subfigure 13.4: RANS ($k-\zeta-f$) – turbulence kinetic energy

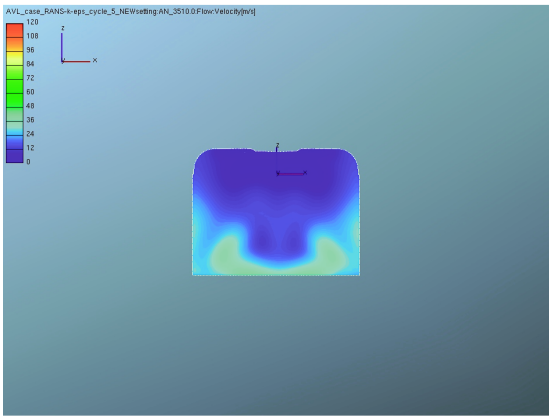

Subfigure 13.5: RANS ($k-\epsilon$) – velocity magnitude

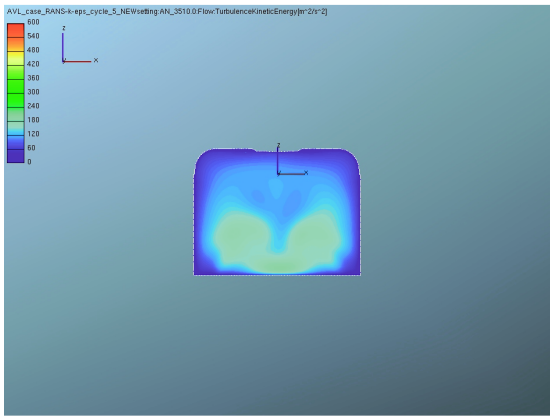

Subfigure 13.6: RANS ($k-\epsilon$) – turbulence kinetic energy

Figure 13: Comparison of different turbulence models at crank angle of 630 degCA (early compression stroke) – averaged velocity magnitude is plotted in left column while turbulence kinetic energy is placed in right column (cutting plane perpendicular to Y-axis – see Figure 1 for coordination system orientation).

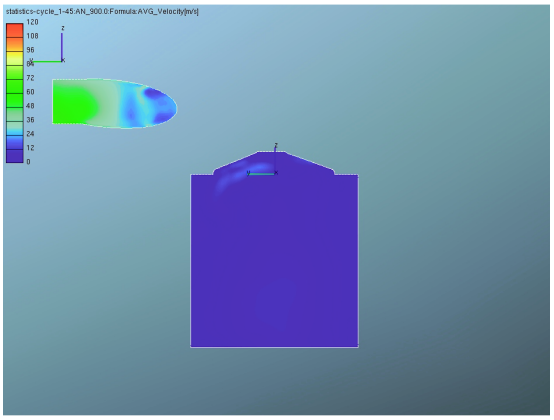

Subfigure 14.1: LES (Smagorinsky) – averaged velocity magnitude

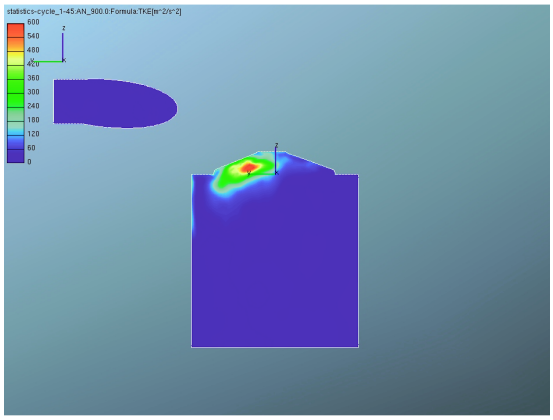

Subfigure 14.2: LES (Smagorinsky) – averaged turbulence kinetic energy

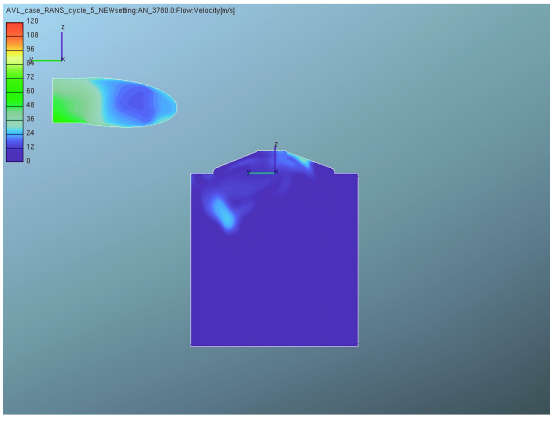

Subfigure 14.3: RANS ($k-\zeta-f$) – velocity magnitude

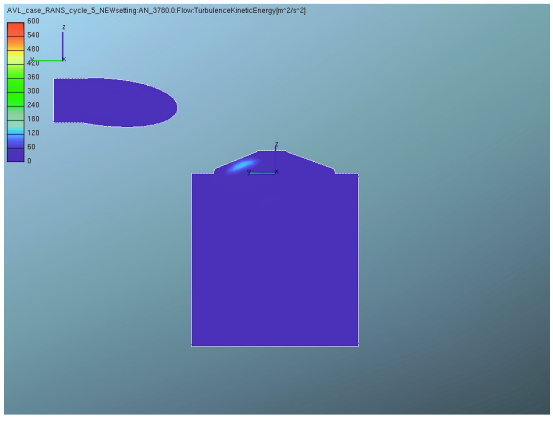

Subfigure 14.4: RANS ($k-\zeta-f$) – turbulence kinetic energy

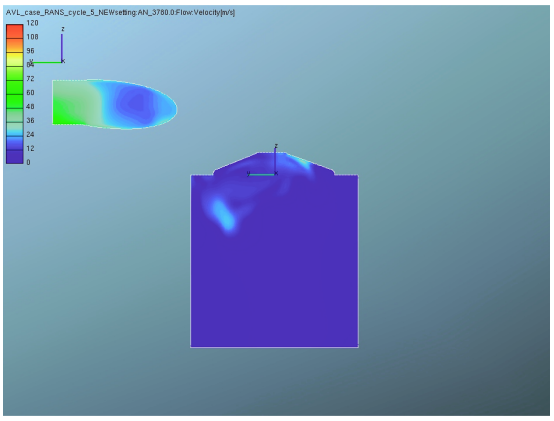

Subfigure 14.5: RANS ($k-\epsilon$) – velocity magnitude

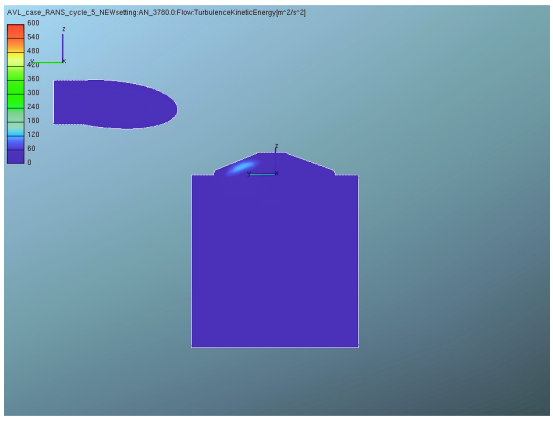

Subfigure 14.6: RANS ($k-\epsilon$) – turbulence kinetic energy

Figure 14: Comparison of different turbulence models at crank angle of 900 degCA (early exhaust stroke) – averaged velocity magnitude is plotted in left column while turbulence kinetic energy is placed in right column (cutting plane perpendicular to X-axis – see Figure 1 for coordination system orientation).

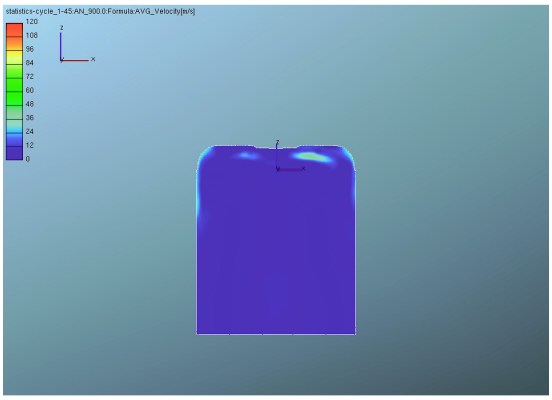

Subfigure 15.1: LES (Smagorinsky) – averaged velocity magnitude

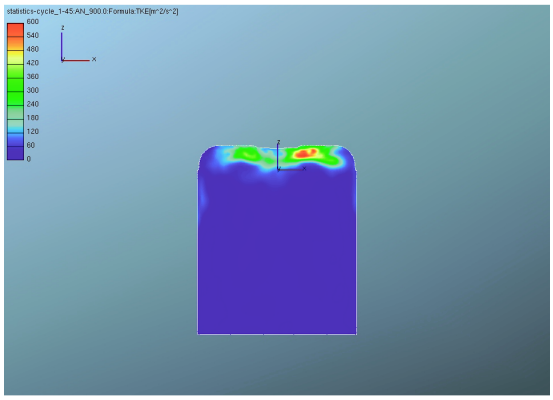

Subfigure 15.2: LES (Smagorinsky) – averaged turbulence kinetic energy

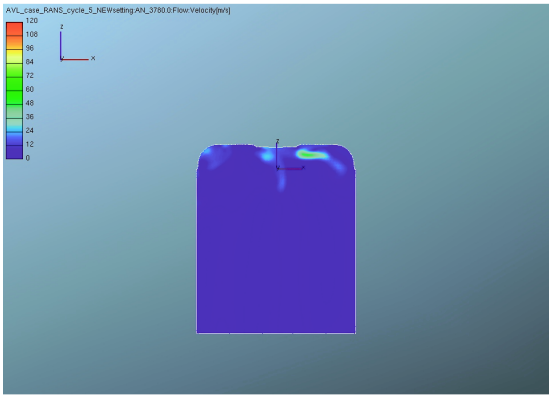

Subfigure 15.3: RANS ($k-\zeta-f$) – velocity magnitude

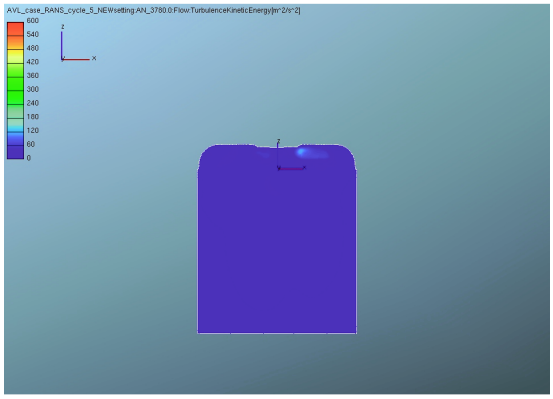

Subfigure 15.4: RANS ($k-\zeta-f$) – turbulence kinetic energy

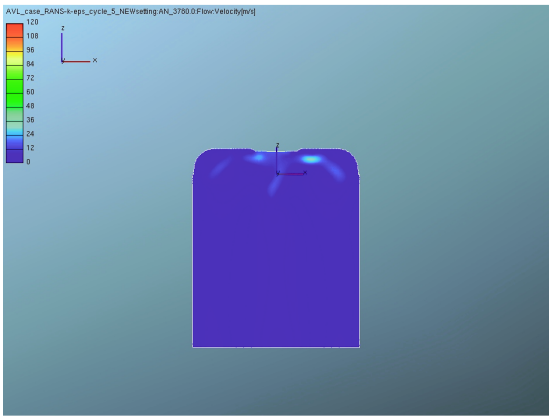

Subfigure 15.5: RANS ($k-\epsilon$) – velocity magnitude

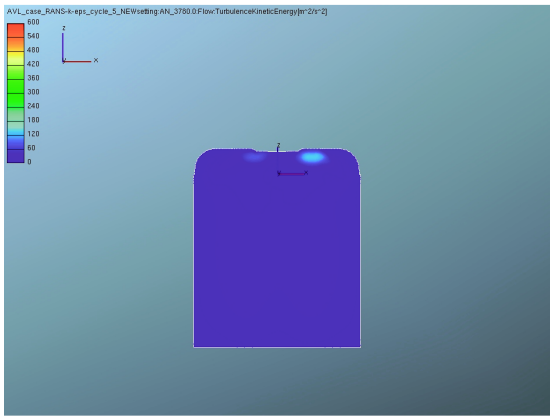

Subfigure 15.6: RANS ($k-\epsilon$) – turbulence kinetic energy

Figure 15: Comparison of different turbulence models at crank angle of 900 degCA (early exhaust stroke) – averaged velocity magnitude is plotted in left column while turbulence kinetic energy is placed in right column (cutting plane perpendicular to Y-axis – see Figure 1 for coordination system orientation).

5 Conclusion

The presented work is based on comparison of different approaches to turbulence modelling for the case of motored 4-stroke internal combustion engine (ICE). The first approach uses simple LES model (Smagorinsky) and ensemble averaging. The second one applies classical RANS models ($k-\zeta-f$, which is recommended by AVL for ICE applications in FIRE code, and standard $k-\epsilon$). This is purely theoretical study – no experimental data are available. Hence, only qualitative comparison is possible. However, it is reasonable to assume that LES should have the best predictive ability (as the mesh size, time step and numerical accuracy are no too off the recommended values for 'proper' LES simulation) of all tested turbulence models.

The first set of presented results deals with LES and its statistical evaluation applying ensemble averaging. As each LES engine cycle represents one realization of a particular experiment (the previous cycle directly influences the following one), it is necessary to calculate many consecutive cycles. Then an ensemble averaging modified for periodic phenomena is applied to obtain averaged values and fluctuation ones. Such approach is clearly very time consuming, however there is a lot of information avaliable. One important issue is how many engine cycles need to be calculated to get statistically converged results. It seems that 25 cycles are needed to obtain convergence for the statistical moments of the 1st-order (e.g. averaged velocity field) while at least 40 cycles have to be calculated to get converged moments of the 2nd-order (e.g. turbulence kinetic energy). This conclusion cannot be generalized as it is based on results concerning one engine operation point only. However, these conclusions seem to be consistent with the well-known knowledge of other researchers dealing with application of LES to ICEs.

The second set of results concerns the comparison of LES and RANS. The main conclusion is that the averaged velocity vector magnitude fields are relatively similar. On the other hand, the same cannot be stated for turbulence kinetic energy ones. It seems that LES predicts significantly higher values of that. When comparing both RANS models (AVL's recommended $k-\zeta-f$ and standard $k-\epsilon$), they are relatively similar. The standard $k-\epsilon$ predicts a bit higher peaks of turbulence kinetic energy and it has a faster tendency to return to symmetry once the geometry is symmetrical.

From practical point of view, the LES is still far too time consuming while the requirements for computer power and data storage are very demanding. The necessity to perform statistical evaluation (in other words – to calculate many consecutive cycles) is mainly responsible for that. However, it seems to be a promising approach to significantly improve predictive ability of CFD tools, especially during early stages of design phase when little experimental data are available.

Final comment regards comparison with experimental data – it is in progress within EU project LESSCCV (started December 2009, it ends December 2012). It is expected that first results will be available before the end of the year 2010. No instantaneous velocity vector fields are supposed to be measured – instead, the indirect comparison have to be made using in-cylinder pressure traces. Moreover, the engine will be operated in 'normal' SI mode – both fuel injection (directly into a cylinder) and combustion (turbulent flame front propagation) have to be taken into account. Based on that, the presented work can be

considered as the first step before adding LES-ready models for a spray and combustion. It is clear that application of LES to ICE is very challenging – however, expected benefits are worth trying that.

Acknowledgement

This work has been supported within the MŠMT project COST OC 167 "Numerical Simulation in Internal Aerodynamics using LES or LES/RANS Methods". This help is gratefully appreciated.

Additional support was received by the Josef Božek Research Center, No. 1M68400770002. This help has also been gratefully appreciated.

References

[1] *Fire 2009.SP1 [DVD]*. AVL List GmbH, 2009.

[2] Basara, B., Schneider, J., and Baier, W. *AVL's New Standards for Modelling Turbulence in Automotive Flows. In: XXI Intl. JUMV Automotive Conference SCIENCE & MOTOR VEHICLES, Beograd*, pages 1–11, 2007. NMV0721.

[3] Celik, I., Yavuz, I., and Smirnov, A. *Large Eddy Simulations of In-cylinder Turbulence for Internal Combustion Engines: a Review*. *International Journal of Engine Research*, Vol. 2(2):119–148, 2001. ISSN 1468-0874.

[4] Girimaji, S. S. *Partially-Averaged Navier-Stokes Model for Turbulence: A Reynolds-Averaged Navier-Stokes to Direct Numerical Simulation Bridging Method*. *J. Appl. Mech.*, Vol. 73(3):413–421, May 2006.

[5] Girimaji, S. S., Jeong, E., and Srinivasan, R. *Partially Averaged Navier-Stokes Method for Turbulence: Fixed Point Analysis and Comparison with Unsteady Partially Averaged Navier-Stokes*. *J. Appl. Mech.*, Vol. 73(3):422–429, May 2006.

[6] Hanjalić, K., Popovac, M., and Hadžiabdić, M. *A Robust Near-wall Elliptic-relaxation Eddy-viscosity Turbulence Model for CFD*. *Int. J. of Heat and Fluid Flow*, Vol. 25:1047–1051, 2004.

[7] Haworth, D. C. *Large Eddy Simulations of In-cylinder Flows*. *Oil and Gas Sci. Technol. Rev., IFP*, Vol. 54(2):175–185, 1999.

[8] Launder, B. E. and Sharama, B. I. *Application of the Energy Dissipation Model of Turbulence to the Calculation of Flow Near a Spinning Disc*. *Letters in Heat and Mass Transfer*, Vol. 1(2):131–138, 1974.

[9] Launder, B. E. and Spalding, D. B. *Mathematical Models of Turbulence*. *Academic Press, London*, 1972.

[10] Lesieur, M., Métais, O., and Comte, P. *Large-Eddy Simulations of Turbulence*. Cambridge University Press, 40 West 20th Street, New York, NY 10011-4211, USA, 2005. ISBN 0-521-78124-8.

[11] Naitoh, K., Itoh, T., and Takagi, Y. *Large Eddy Simulations of Premixed Flame in Engine Based on the Multilevel Formulation and the Renormalization Group Theory*. *SAE Technical Paper Series*, February 1992. Paper 920590.

[12] Sagaut, P. *Large Eddy Simulation for Incompressible Flows*. Scientific Computation. Springer Berlin Heidelberg New York, 3. edition, 2006. ISBN 3-540-26344-6.

[13] Smagorinsky, J. *General Circulation Experiments with the Primitive Equations*. *Mon. Weather Rev.*, Vol. 91(3):99–164, 1963.

[14] Smirnov, A., Yavuz, I., and Celik, I. *Diesel Combustion and LES of In-Cylinder Turbulence for IC-Engines*. *In: ASME Fall Technical Conference on In-Cylinder Flows and Combustion Processes, Ann Arbor, Michigan*, pages 119–127, 1999. Paper 99-ICE-247.

[15] Wilcox, D. C. *Reassessment of the Scale Determining Equation for Advanced Turbulence Models*. *AIAA Journal*, Vol. 26(11):1299–1310, 1988.

[16] Yavuz, I. and Celik, I. *Turbulence Generation Mechanisms in IC-Engine Flows: A Numerical Study*. *In: Conference on Thermo-fluid-dynamics, Processes in Diesel Engines, THIESEL '2000, Valencia, Spain*, September 2000.